Journal of Optoelectronics and Advanced Materials Vol. 2, No. 2, June 2000, p. 139 - 145

ON THE ROLE PLAYED BY THE SILICON SUBSTRATE IN THE CRYSTALLIZATION, PHOTO-VITRIFICATION AND PHOTO-OXIDATION OF $As_{50}Se_{50}$ LAYERS

R. Prieto-Alcón, E. Márquez, J. M. González-Leal

Departamento de Física de la Materia Condensada, Facultad de Ciencias
Universidad de Cádiz, 11510 – Puerto Real (Cádiz), Spain

The role played by the silicon substrate in the light-induced vitrification of $As_{50}Se_{50}$ thin films is analyzed. It is demonstrated that these films can crystallize into different structures, depending on the substrate they are attached to. Photo-oxidation when the illuminated film is deposited on silicon can be enhanced due to a chemical reaction of the chalcogenide material with Si, which produces arsenic that would be then oxidized. The spectral irradiance of the light source employed also influences the photo-amorphization phenomenon, because the existence of a larger proportion of photons with higher energy will probably cause a larger degree of disorder in the films. Finally, the reversible structural changes induced by light in $As_{50}Se_{50}$ layers are accompanied by reversible photo-darkening.

(Received May 18, 2000; accepted May 29, 2000)

Keywords: Amorphous chalcogenide, Photo-vitrification, Photo-oxidation, Arsenic Selenide, X-ray diffraction, Crystallization, Far-infrared spectrum

1. Introduction

Amorphous chalcogenides can undergo various photo-induced structural changes [1-5]. Usually, the amorphous chalcogenides are deposited on glass or silicon wafers. In many cases the effects induced by light or other factors mechanical, thermal, electrons, nuclear particles etc., have been studied on thin films deposited on such substrates. After our knowledge no studies regarding the effect of substrates on the amorphous chalcogenide films (structure and light induced properties) have been carried out up to day. In this work, we report, mainly, the results of a study of the differences between photo-vitrification of $As_{50}Se_{50}$ thin films deposited on glass and silicon substrates.

2. Experiments and results

$As_{50}Se_{50}$ thin films were deposited onto glass and silicon substrates using a standard vacuum-evaporation technique. Detailed description of the experimental procedure is given elsewhere [6,7]. Experimental details of the treatments the samples were subjected to, can be found in Ref. [7].

Although most chalcogenide glasses are quite reluctant to crystallization, $As_{50}Se_{50}$ thin films deposited on either glass or silicon substrates, can be crystallized by thermal annealing at $\approx$ 150 °C for around 72 h. The X-ray diffraction (XRD) patterns of our $As_{50}Se_{50}$ films are presented in Figs. 1 and 2.

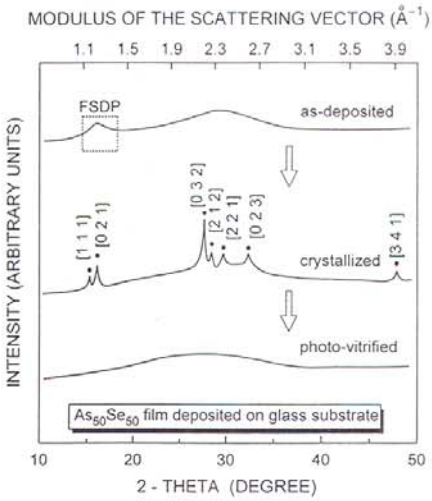

Fig. 1. XRD patterns (Cu Kα radiation) of the as-deposited, crystallized and photo-amorphized $As_{50}Se_{50}$ thin films on a glass substrate.

In addition, Table 1 shows the positions of the most intense XRD peaks for crystallized layers of the already mentioned composition. It is observed that many more peaks are clearly resolved in the case of $As_{50}Se_{50}$ films crystallized onto silicon substrates. On the other hand, comparison of the XRD patterns of the crystallized films with powder-diffraction data for As-Se crystals [8], revealed that the crystalline phase is As_4Se_4. It is important to note the absence of the first sharp diffraction peak (FSDP) at $2\theta \approx 17°$, characteristic of the amorphous phase, in the crystallized products. The influence of medium-range order has been claimed to be responsible for that particular feature of the diffraction results on amorphous chalcogenide materials [9]. Possible preferred orientational effects in the crystallized films are suggested on the basis of the different peak intensities measured in our experiments, compared to the reference powder-diffraction data. Such orientational effects, along with the extent of crystallization, have been shown to be dependent on the $As_{50}Se_{50}$ film thickness, when glass is the substrate used [10].

Table 1. Positions of the most intense XRD peaks (Cu Kα radiation) for crystallized samples of $As_{50}Se_{50}$ deposited onto glass and silicon substrates. Peak positions for As_4Se_4 crystals (ASTM 26 - 122) are given for comparison. Values in parentheses are relative intensities of the peaks.

Interplanar distances d (Å) calculated from the positions of the X-ray diffraction peaks		
glass substrate	silicon substrate	As_4Se_4
5.797 (47)	5.791 (36)	5.870 (30)
5.482 (100)	5.491 (100)	5.560 (50)
3.239 (98)	3.240 (80)	3.260 (95)
3.129 (38)	3.129 (21)	3.140 (40)
2.993 (23)	2.988 (24)	3.000 (95)
2.748 (23)	2.749 (24)	2.790 (100)
1.897 (4)	1.952 (8)	1.900 (45)
	3.814 (6)	3.830 (8)
	2.714 (33)	2.650 (25)
	2.579 (12)	2.580 (35)
2.235 (16)	2.234 (6)	2.240 (30)
	2.167 (3)	2.180 (25)

Our film thicknesses, in the range 700 ÷ 1200 nm, correspond to the medium-thickness case of Ref. [10]. Thus, we can certainly assume that the crystallization process, which takes place upon annealing of medium-thickness $As_{50}Se_{50}$ films, is somewhat different, depending on the type of substrate involved. Furthermore, the different crystallization behaviour observed with films on a substrate, on the one hand, and scraped films and powdered glass, on the other, clearly indicates that there is a very important role played by the film-substrate interface, and mechanical strain is very probably involved. In fact, crystallization might be enhanced by crystallization centres on Si wafers, or by a thin layer of $SiSe_2$ formed at the interface between amorphous chalcogenide and silicon.

It is known that a thin chalcogenide film prepared by thermal evaporation consists of molecular clusters with both heteropolar and homopolar bonds. When the as-evaporated film is annealed, homopolar bonds are broken and energetically more favourable heteropolar bonds are formed instead. The fact that the layer is in contact with the substrate during the annealing procedure, leads to an accumulation of mechanical strain in the layer because the lattice parameters of the chalcogenide film and those of the substrate, as well as their thermal expansion coefficients, are, generally, different. Studies of the influence of the annealing and illumination on vitreous chalcogenide layers, by means of differential scanning calorimetry, have also shown that large mechanical strains were accumulated in a layer annealed on a substrate [11].

The crystallized $As_{50}Se_{50}$ layers were subsequently exposed, in air, to white light from a mercury arc lamp for a period of time of about 10 h, at room temperature, which caused the complete disappearance of the crystalline features in the corresponding XRD pattern (see Figs.1 and 2). This observation obviously implies the photo-amorphization of the present $As_{50}Se_{50}$ films, whether they are deposited onto glass or silicon wafer substrates.

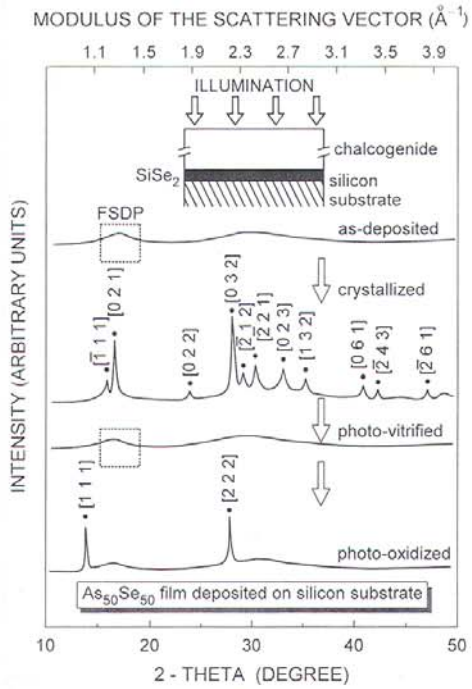

Fig. 2. XRD patterns (Cu Kα radiation) of the as-deposited, crystallized, photo-vitrified and photo-oxidized $As_{50}Se_{50}$ thin films onto silicon wafer substrate. The inset is a schematic representation of the annealed sample being illuminated, showing the possible formation of a thin layer of $SiSe_2$ at the interface of the amorphous-chalcogenide with Si.

A thermocouple conveniently affixed to the surface of the samples enabled us to determine the temperature increase during the irradiation. This increase was never more than ≈ 25 °C, which proves the athermal character of the photo-induced vitrification phenomenon. Interestingly, this temperature increase represents an advantage because, considering that the photo-amorphization was found to be thermally activated [12], with activation energy ΔE_{ph} = 0.15 eV, the illumination time necessary to vitrify the film is reduced by around 35%.

Therefore, in the particular case, which is presented here, the film can even crystallize on annealing near T_g, as it has been demonstrated above, but the mechanical strain present is so strong that on subsequent illumination the film becomes amorphous again. Thus, in an annealed and chemically and structurally more ordered film there are regions with large mechanical strains. Most likely these regions will occur in places where initially homopolar As-As bonds were present, since it was there that the bond switching, and hence the atomic displacements, took place. Should now the annealed film be illuminated, the bonds will weaken and the structure will be able to relax. Since the strain originated from As-As to As-Se bond conversion on annealing, it is probably that As-As bonds will be formed again, this probability being higher at the sites where these As-As bonds were initially present.

3. Disscusion

It is remarkable that, the FSDP is absent from the XRD pattern of the photo-vitrified $As_{50}Se_{50}$ film deposited onto a glass substrate, whereas the corresponding XRD pattern of the light-amorphized $As_{50}Se_{50}$ film deposited onto a silicon substrate contains that feature, although somewhat it has become broader. The type of irradiation affects also the photo-vitrification phenomenon of $As_{50}Se_{50}$ crystallized films [6]. In fact, when a quartz-tungsten halogen (QTH) lamp is used [12,13], the corresponding XRD patterns of as-evaporated and photo-vitrified $As_{50}Se_{50}$ films, deposited onto glass substrates, show no significant difference with respect to their features, including the FSDP. We think that due to much higher UV light content of the mercury lamp compared to the QTH lamp, the former can be expected to produce a larger degree of disorder in the chalcogenide material.

The crystallization-vitrification cycle was found to be reversible with both types of substrates used in this work. That means that the photo-vitrified film, could again be crystallized by thermal annealing at ≈ 150 °C, and then, vitrified once more by the corresponding illumination. We have performed three such cycles on a representative sample, with both types of substrates.

On the other hand, in the course of the vitrification of an $As_{50}Se_{50}$ film deposited on a silicon substrate, photo-oxidation of the film has been additionally detected. Arsenic trioxide micro-crystals were formed in the whole matrix of the film [6]. Such oxidation has not been observed with $As_{50}Se_{50}$ films deposited on glass substrates. The enhanced oxidation of $As_{50}Se_{50}$ on Si wafers can be connected with the fact that on the interface of the amorphous chalcogenide with Si, the following chemical reaction (possibly enhanced by illumination) can take place:

$$As_4Se_4 + 2\,Si \rightarrow 2\,SiSe_2 + 4\,As, \quad (1)$$

and created arsenic is then more easily oxidized, according to:

$$4\,As + 3\,O_2 \rightarrow 2\,As_2O_3. \quad (2)$$

Reaction (1) can also proceed during annealing. Either $SiSe_2$ or Si can form crystallization centres, which result in a more pronounced X-ray pattern.

Typical far-infrared transmission spectra for as-deposited, crystallized and photo-amorphized $As_{50}Se_{50}$ films, onto silicon wafer substrates, are shown in Fig. 3. Assignment of the main infrared features is summarized in Table 2.

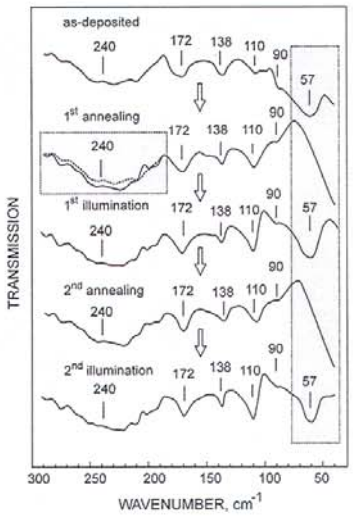

Fig. 3. Far-infrared spectra for the as-deposited, crystallized and photo-amorphized $As_{50}Se_{50}$ samples, along with those for the crystallized and photo-vitrified $As_{50}Se_{50}$ samples, corresponding to a second cycle. There is a box showing how the main chalcogenide stretch peak has increased as a consequence of the first thermal annealing.

Table 2. Assignment of the main IR-features of virgin (V), annealed (A), photo-vitrified (PV) and photo-oxidized (PO) $As_{50}Se_{50}$ films.

IR-feature (cm^{-1})	State of the film	Idealized Structural Unit	Reference
240	V, A, PV	$AsSe_3$, As_2Se_3	[8]
172	V, A, PV		[9]
138	V, A, PV	Se_n chains	[10]
110	V, A, PV	$AsSe_3$, As_2Se_3	[11]
90	V, A, PV	Se_8 rings	[10]
57	V, PV		
620	PO	As_2O_3	[12]

Although in $As_{50}Se_{50}$ there are prevailing As_4Se_4 molecules, it is reasonable to suppose that during evaporation, the following reactions proceed:

$$2\ As_4Se_4 \rightarrow 2\ As_2Se_3 + As_4 + Se_2 \quad (3)$$

or

$$3\ As_4Se_4 \rightarrow 4\ As_2Se_3 + As_4 \quad (4)$$

Se_2 can then be polymerized to Se_n chains. From those chemical reactions, it is clear that there should be excess of As or As plus Se, which would lead to the presence of As-As bond vibrations in the corresponding IR transmission spectra. Nevertheless, the difference between atomic weights of As and Se is low and the vibration frequencies of As-As, As-Se and Se-Se bonds in similar structural

units are very close. The overlapping of their vibrations can be strong, especially in amorphous solids with broader IR bands, and, therefore, it is difficult to separate them and assign the vibrations to the individual modes. The IR spectrum of the crystallized $As_{50}Se_{50}$ film shows the existence of bands at wavenumbers very close, indeed, to those already found in the spectrum of the as-deposited sample. Nevertheless, there is an outstanding difference between those IR transmission spectra: the complete disappearance of the vibrational band at 57 cm^{-1}, as a consequence of the thermal annealing. In addition, the main chalcogenide stretch band seems to increase (see Fig. 3, in which a box has been drawn to highlight this observation), indicating an increase in the As-Se bond density, as a result of the ordering of the film, induced by the corresponding thermal annealing.

Illumination of the crystallized $As_{50}Se_{50}$ sample with a Hg arc lamp gives rise to the presence again of the absorption band at 57 cm^{-1} in the IR spectrum of the corresponding exposed sample. The absorption bands assigned to As-Se bond vibrations, and those attributed to Se_n chains and Se_8 rings, which were observed in the spectra of both, the as-deposited and crystallized $As_{50}Se_{50}$ films, are also present in the photo-vitrified sample spectrum. Next, the $As_{50}Se_{50}$ film was subjected to a second annealing followed by a second illumination treatment. The vibrational bands observed in the far-IR spectra for the crystallized and photo-vitrified layers, corresponding to the second annealing-illumination cycle, are also displayed in Fig. 3. From the above results, we can conclude that there is a very clear change in the vibrational band at 57 cm^{-1}, whereas the other bands remain practically unchanged. This vibrational band could be connected with some intramolecular or lattice (blocks in amorphous solids) vibrations, although the first reason is more probable. The bending vibrations can not be excluded either.

Finally, the crystalline structure of the annealed $As_{50}Se_{50}$ film is composed of As_4Se_4 molecules. These molecules have a cage-like structure, in which a square of Se atoms bisects a distorted tetrahedron of As atoms (Fig. 4). The average As-As bond length in As_4Se_4 is 2.57 Å, and the As-As-Se bond angle subtended at either one of the As atoms comprising the As-As bonds is 101.2°. If one compare those values with the corresponding bond distance and bond angle in *a*-As, 2.49 Å and 98°, respectively, it is found that they are larger in the case of the As_4Se_4 molecule. The intermolecular distances, less than 3.70 Å, are shorter than the predicted van der Waals distance of 4.0Å, which could be associated with relatively strong intermolecular interactions. Since the present light-induced amorphization phenomenon is athermal, the action of the photons must certainly be to cause chemical bond breaking.

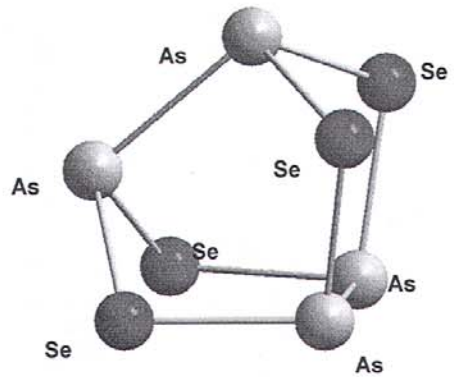

Fig. 4. Crystal and molecular structure of tetrameric arsenic selenide As_4Se_4.

A possible mechanism to explain the phenomenon would involve intramolecular bond breaking of covalent bonds within the As_4Se_4 molecular units, to yield a cross-linked amorphous network. Nevertheless, there is another possibility, which would maintain the integrity of the As_4Se_4 molecules, although changes in their relative orientation and spatial distribution would occur, as a consequence of photo-induced intermolecular bond breaking. It has been suggested [14] that, since As-As distances and bond angles in As_4Se_4 are quite different from those in pure As, as clearly seen above, one can conclude that such intramolecular As-As bonds are rather strained. As a result, the electronic states associated with these particular chemical bonds are likely to be at, or just above, the

top of the valence band. Thus, optical illumination might be expected, preferentially, to involve the excitation of such electronic states, leading to bond cleavage; As-Se bond formation could then occur between closest atoms of neighboring molecules, leading to a more cross-linked and disordered structure. In addition, intramolecular As-Se bonds may also be broken upon irradiation, giving rise to intermolecular As-Se bond formation.

Details of an optical study of the athermal photo-amorphization can be found in our previous works [7,15]. The values of the optical gap lead us to the conclusion that a clear reversible photo-darkening process accompanies the present photo-induced vitrification phenomenon. This conclusion is clearly supported by the above-mentioned FIR results. It is well known that As-As bonds play an important, although not predominant, role in reversible photo-darkening in well-annealed As-rich chalcogenide samples [2,3]. An increase in the As-As bond concentration, as a consequence of illumination, leads to a decrease of the optical gap, owing to formation of electronic states associated with such bonds, at, or just above, the top of the valence band. Similarly, the subsequent annealing of the sample will lead to a decrease in the As-As bond concentration, and therefore, to an increase of the optical gap, because breaking of As-As bonds will replace electronic states in the gap associated with these homopolar bonds, by non-bonding As states located near the conduction band edge.

4. Conclusions

The processes of crystallization and photo-oxidation of chalcogenide$As_{50}Se_{50}$ films are significantly influenced by the substrate. Silicon plays an active role during illumination. An enhanced effect of photo-oxidation due to substrate was demonstrated.

Acknowledgements

This work was supported by the CICYT (Spain), under the MAT98-0791 project.

References

[1] J. S. Berkes, S. W. Ing, W. J. Hillegas, J. Appl. Phys., **42**, 4908 (1971).
[2] S. R. Elliott, J. Non-Cryst. Solids, **81**, 71 (1986).
[3] G. Pfeiffer, M. A. Paesler, S. C. Agarwal, J. Non-Cryst. Solids, **130**, 111 (1991).
[4] P. J. S. Ewen, A. E. Owen, en: "High-Performance Glasses", eds. M. Cable, J.M. Parker (Blackie, Londres, 1992).
[5] L. Tichý, A. Vidourek, P. Nagels, R. Callaerts, H. Tichá, Opt. Mater., **10**, 117 (1998).
[6] R. Prieto-Alcón, J. M. González-Leal, A. M. Bernal-Oliva, E. Márquez, Mater. Lett., **36**, 157 (1998).
[7] R. Prieto-Alcón, E. Márquez, J. M. González-Leal, R. Jiménez-Garay, A.V. Kolobov, M. Frumar, Appl. Phys., **A 68**, 1 (1999).
[8] Powder Diffraction File, Inorganic Phases, JCPDS International Centre for Diffraction Data, 1988.
[9] S. R. Elliott, Phys. Rev. Lett., **67**, 711 (1991).
[10] A. V. Kolobov, S. R. Elliott, Philos. Mag., **B 71**, 1 (1995).
[11] V. A. Bershtein, L. M. Egorova, S. R. Elliott, A. V. Kolobov, Proc. of the XVI International Congress on Glass, J. M. Fernández Navarro ed. (Sociedad Española de Cerámica y Vidrio, Madrid, 1992) p. 285.
[12] S. R. Elliott, A. V. Kolobov, J. Non-Cryst. Solids, **128**, 216 (1991).
[13] A. V. Kolobov, V. A. Bershtein, S. R. Elliott, J. Non-Cryst. Solids, **150**, 116 (1992).
[14] A. V. Kolobov, S. R. Elliott, J. Non-Cryst. Solids, **189**, 297 (1995).
[15] C. Corrales, J.B. Ramírez-Malo, E. Márquez, R. Jiménez-Garay, Mater. Sci. Eng. B-Solid, **47** 119 (1997).